Efficiency and stability evaluation of Cu_2O/MWCNTs filters for virus removal from water

K. Domagała*[a,b], C. Jacquin[c], M. Borlaf[a], B. Sinnet[c], T. Julian[d,e,f], D. Kata[b], T. Graule[a]

[a]*Laboratory for High Performance Ceramics, Empa, Swiss Federal Laboratories for Materials Science and Technology, Dübendorf, Switzerland*

[b]*Faculty of Materials Science and Ceramics, AGH, University of Science and Technology, Krakow, Poland*

[c]*Department of Process Engineering, Eawag, Swiss Federal Institute of Aquatic Science and Technology, Dübendorf, Switzerland*

[d]*Department Environmental Microbiology, Eawag, Swiss Federal Institute of Aquatic Science and Technology, Dübendorf, Switzerland*

[e]*Swiss Tropical and Public Health Institute, Basel, Switzerland*

[f]*University of Basel, Basel, Switzerland*

** Corresponding author: kamila.domagala@empa.ch, +41 58 765 4308*

Abstract:

Both multi-walled carbon nanotubes (MWCNTs) and metal or metal oxides have demonstrated virus removal efficacy in drinking water applications. In this study, MWCNTs were coated with copper(I) oxide (Cu_2O) using three distinct synthesis procedures (copper ion attachment, copper hydroxide precipitation, and $[Cu(NH_3)_4]^{2+}$ complex attachment) and virus removal efficacy (using MS2 bacteriophages) was evaluated. All synthesis procedures resulted in the presence of adsorbed, nanosized Cu_2O particles on the MWCNTs, shown using X-ray diffraction. Further, transmission electron microscopy confirmed uniform copper(I) oxide distribution along the MWCNTs for all three materials. Virus removal efficacy was assessed for all three synthesised composites both before and after material conditioning (filtering for at least 24 h/ 280 mL/h), and accounting for additional MS2 inactivation in the permeate due to continued copper inac-

tivation from dissolved/desorbed copper in permeate (time-control). Material conditioning influenced virus removal, with the first litres of water containing higher concentrations of copper than the sixth litres of water, suggesting excess or non-bonded copper species dissolve from filters. Higher copper dissolution was observed for water at pH 5 than at pH 7, which decreased with time. Copper dissolution most likely caused an associated decrease in copper adsorbed to MWCNTs in the filters, which may explain the observed lower MS2 removal efficacy after conditioning. Additionally, the time-control study (immediately after filtration as compared to two hours after filtration) highlighted continued MS2 inactivation in the permeate over time. The obtained results indicate that the synthesis procedure influences virus removal efficacy for MWCNTs coated with copper oxides and that virus removal is likely due to not only virus electrostatic adsorption to the coated MWCNTs, but also through antiviral properties of copper which continues to act in the permeate. In conclusion, it is highly important to revise the methods of testing filter materials for virus removal, as well as procedure for virus concentration evaluation.

Keywords: virus removal, MS2, MWCNT, copper(I) oxide, conditioning, copper dissolution

1. Introduction

An estimated 29% of the global population currently lacks access to safely managed drinking water services (UNICEF and WHO, 2019). Unsafe drinking water contributes to the spread of waterborne illnesses, including diarrheal diseases, which are responsible for an estimated 700'000 child deaths per year (Fischer Walker et al., 2013; Liu et al., 2015). In this context, sustainable, low cost, effective, and decentralised water treatment technologies could help to improve water quality globally. In well operated and equipped decentralised systems, bacteria and protozoa removal is readily achievable, but virus removal is difficult remaining a major challenge (Gibson et al., 2011). The physical removal of viruses is complicated due to their size. Granulated Activated Carbon (GAC) is largely ineffective and filtration requires membranes with sufficiently small pore sizes (i.e., nanofiltration or reverse osmosis) (Altintas et al., 2015; Gall et al., 2015; Shimabuku et al., 2017). Disinfectants (i.e., UV light, chlorine, chloramines) are common, however, they are inhibited by high costs of operation and maintenance, reliance on a supply chain and end user preferences (Crider et al., 2018; Lantagne and Clasen, 2013). More specifically, the use of chemical oxidants or UV requires additional consumables, access to which may be restricted in remote areas, generates disinfection by-products and is not always efficient for virus removal (Sirikanchana et al., 2008; WHO, 2017). Therefore, there is a need for new, low cost, low maintenance, sustainable technologies capable of improved virus removal without the necessity of additional consumables at the household scale (e.g., meeting the US Environmental Protection Agency standards for drinking water of 4 Log_{10} Removal Value (LRV)) (Peter-Varbanets et al., 2009; Rahaman et al., 2012; United States Environmental Protection Agency, n.d.).

It should be noted that the manufacturing of carbon nanotubes (CNTs) becoming to be "greener", while retaining process efficiency, mitigating environmental impact and the production of side-products (Trompeta et al., 2016). Production costs are also decreasing. The price

per gram in the year 2000 was $150 and decreased to $50 in 2010 (Wood, 2018). Nowadays, it is possible to buy carbon nanotubes even for a few dollars per gram. Furthermore, copper (material used for CNTs modification) exists in abundance and is relatively cheap in comparison to other metals, such as silver. In this context, carbon nanotubes are a promising filter material, due to their high surface area and sorption capacity (Elsehly et al., 2018; Ong et al., 2010; Sarkar et al., 2018). Moreover, their needle-like shapes form entangled layers, decreasing effective membrane pore size and potentially increases virus retention without impairing filter flux (Brady-Estévez et al., 2010). Several prior studies have shown that filters prepared with CNTs effectively remove MS2 bacteriophages, a commonly used surrogate for enteric viruses. For example, Brady-Estévez et al. (2010) showed that polyvinylidene fluoride (PVDF) membranes (5 µm) coated with a 2 mm MWCNTs layer reached between 5 and 8 LRV, depending on the filtration conditions (Brady-Estévez et al., 2010).

One challenge of using MWCNTs for virus filtration, however, is virus retention. Although Rahaman et al. (2012) presented sufficient virus removal, 10^4 Plaque Forming Units (PFU/mL) of MS2 subsequently desorbed from the filter, showing that pristine MWCNTs are not enough to ensure virus-free water production (Rahaman et al., 2012). Functionalising MWCNTs might improve their antiviral properties. MWCNT functionalisation with metals and metal oxides is well known, finding applications, such as catalysts gas sensors and supercapacitors (Guo and Li, 2005; Mallakpour and Khadem, 2016; Qin et al., 2000; Rajarao et al., 2014; Satishkumar et al., 2000; Wang et al., 2005; Wani et al., 2016). In the context of virus removal, functionalisation with antimicrobial silver, copper and copper oxides would provide an additional virus removal mechanism. For example, ceramic filters impregnated with colloidal silver or silver nanoparticles are often used to treat drinking water to effectively remove bacteria (though virus removal remains low) (Ngoc Dung et al., 2019; Oyanedel-Craver and Smith, 2008; Salsali et al., 2011; Van der Laan et al., 2014). However, a filter with MWCNTs functionalised with silver showed complete removal of poliovirus, norovirus, and coxsackie virus (Kim et al.,

2016). Nevertheless, the benefits of copper relative to silver include greater virus removal efficacy and reduced costs, which make it more suitable for virus filter development for drinking water treatment (Dankovich and Smith, 2014). In the case of copper, the guideline limit concentration in drinking water set by World Health Organization (WHO) is equal to 2 mg/L, whereas for silver 0.1 mg/L (WHO, 2004a, 2004b).

Németh et al. (2019) demonstrated that Cu_2O-MWCNTs filters are promising for virus removal in drinking water (Németh et al., 2019). Up to 4 LRV was registered after the filtration of MS2 by Cu_2O-MWCNTs filters at pH between 5.0 and 9.0. However, Nemeth et al. (2019) did not measure copper concentration in the permeate after filtration. This parameter is crucial to evaluate the stability of the material (defined here by minimized copper dissolution) and safety of the water produced (Oyanedel-Craver and Smith, 2008; Rao et al., 2016). Related to estimates of copper dissolution, the antiviral properties of copper may contribute to continued virus inactivation in the permeate. Notably, the relative roles of virus removal through the filter (i.e., adsorption, size exclusion) and virucidal activity of dissolved metals is rarely considered (Van der Laan et al., 2014). For example, Dankovich and Smith (2014) demonstrated that CuO-nanoparticle (NP) purifiers performed well in terms of virus removal and that the measured copper concentration in the permeate was lower than the WHO guideline value of <2 mg/L (300 µg/L) (Dankovich and Smith, 2014). Nonetheless, no further tests were performed to evaluate the effect of copper concentration on virus removal in the permeate. Armstrong et al. (2017) demonstrated that there was a 1.8 LRV reduction of MS2 within 6 h in presence of 2 mg/L of $CuCl_2$, which led to the conclusion that time control of virus removal analysis after virus filtration is crucial (Armstrong et al., 2017).

Based on the above-mentioned considerations, the aim of the presented work was to (i) develop Cu_2O/ MWCNTs composites as a filter material and compare three distinct synthesis routes; (ii) evaluate the material stability (defined here as copper dissolution) after conditioning, (iii)

test virus removal performance of the developed materials accounting for continued inactivation of virus in permeate, (iv) evaluate copper concentration in filtrate, (v) examine continued virus inactivation in permeate ("time control") to (vi) discuss possible mechanisms responsible for the virus inactivation/ removal by tested material. To do so, composites were prepared by copper ion attachment, copper hydroxide precipitation and copper complex attachment. Moreover, to distinguish this work from Németh et al (2019), we evaluated three different synthesis routes (Németh et al., 2019). This allowed to obtain filter materials with a more homogeneous distribution of Cu_2O particles on MWCNTs surface, providing more active sites and better access of MS2 bacteriophages to copper(I) oxide particles. The size, metal oxidation state and morphology of the Cu_2O particles, as well as the stability and efficiency of the filters were analysed. The performance of as-prepared filters in terms of MS2 bacteriophages removal was evaluated before and after 24 h (flow through of 6 litres) of filter conditioning at pH 5 and 7. Additionally, the concentration of MS2 in the permeate was tested with time control (checked directly after permeate collection t=0 h, and after two hours t=2 h), followed by copper concentration evaluation in the filtrate to determine the copper dissolution effect on virus removal. Filter material was tested at pH 5-7, due to the importance of this pH range on filter material stability and possible Cu_2O dissolution. This is supported by the increased solubility of Cu_2O at low pH, which may impact MS2 inactivation (Vargas et al., 2017; Z. Wang et al., 2013). The pH of natural waters often exceeds 7, so further testing at higher pH would be required prior to implementation.

2. Materials and methods

2.1. Materials and reagents for Cu_2O/ MWCNTs synthesis

MWCNTs were purchased from Cheap Tubes (outer diameter 10-30 nm, length 10-30 µm, purity> 95 wt. %), copper (II) acetate monohydrate purity≥ 99.0% ($Cu[CH_3COO]_2 \times H_2O$) and ammonium hydroxide 25% (NH_4OH) from Merck. Water purified via MicroPure UV System,

Thermo Scientific (purity 18.2 MΩ), was used for rinsing the MWCNTs, the syntheses of the composites, as well as preparing media for the DAL method.

2.2. Composites synthesis procedures

Copper(I) oxide/ MWCNTs composites were synthesised via three methods: copper ion attachment (route 1), copper hydroxide precipitation (route 2) and $[Cu(NH_3)_4]^{2+}$ complex attachment (route 3). Copper(I) oxide was chosen due to the lower solubility in comparison to copper(II) oxide at the whole pH range (Domagala et al., 2019a; Palmer and Bénézeth, 2008). In all cases, functionalised MWCNTs were used to make the composites.

2.2.1. MWCNTs functionalisation

MWCNTs functionalisation was done by means of a two-step process, according to our previous work (Domagala et al., 2019b). First, MWCNTs (0.01 g/mL) were immersed in 10% HCl at room temperature for 2 h under constant stirring (300 rpm). Then, the MWCNTs suspension was filtered and rinsed with water until the permeate reached pH 7. The collected MWCNTs were subsequently added to 65% HNO_3 (0.01 g/mL) and sonicated for 45 min in a sonication bath filled with ice (DT106, Bandelin Electronics). The suspension was then heated at 120 °C for 4 h under reflux conditions, cooled to room temperature, and washed with water again until pH 7 was reached. Finally, the functionalised MWCNTs were dried overnight in an oven at 120 °C (FD-115, Binderat).

2.2.2. Cu^{2+} ion attachment (composite 1)

Copper acetate hydrate was dissolved in water (0.285 M) and the resulting solution was added to a suspension of functionalised MWCNTs in water (0.2 g/100 mL water, sonicated 10 min in a sonication bath). The addition was carried out under constant stirring (300 rpm) for 2 h. Next, the suspension was filtered (PVDF 0.1 µm, 47 mm, Hawach Scientific) and the solid product

was dried overnight in an oven at 120 °C. A calcination process was performed under N_2 atmosphere at 300 °C for 2 h in a tube furnace (GHC 120900, Carbolite Gero GmbH & Co. KG) to obtain Cu_2O. Figure 1 shows a scheme of the synthesis procedure.

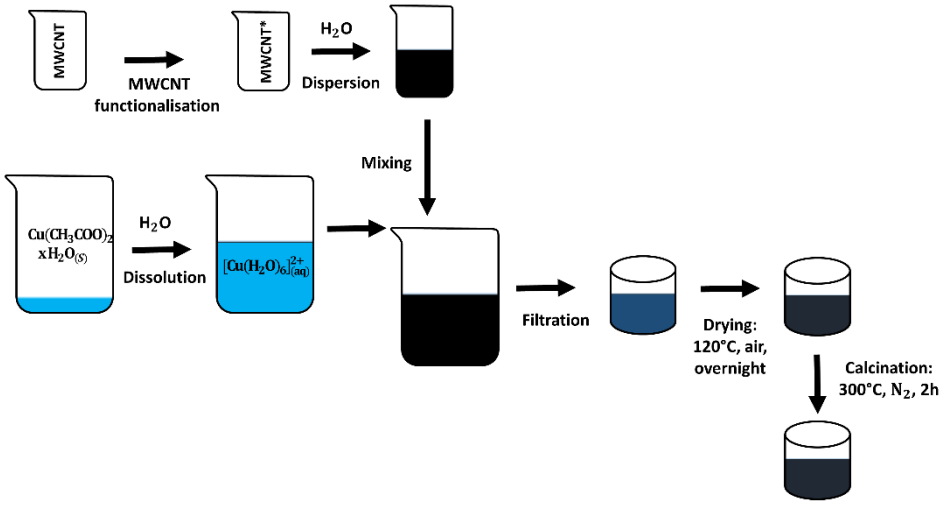

Figure 1. Scheme of the copper ion attachment synthesis (route 1).

2.2.3. Copper hydroxide precipitation (composite 2)

The precursor solution of copper acetate and the dispersion of functionalised MWCNTs were prepared following the same procedure as for the first method. Once both were mixed, an ammonium hydroxide solution was gradually added in a stoichiometric (2 mol NH_4OH) ratio to precipitate the $Cu(OH)_2$. The system was left for 2 h under continuous stirring (300 rpm). The obtained suspension was filtered, and the solid product was dried in an oven overnight at 120 °C. Finally, thermal treatment was performed in a tube furnace for 2 h under N_2 atmosphere at 300 °C to obtain Cu_2O.

2.2.4. Complex ion attachment synthesis (composite 3).

The method for copper hydroxide precipitation (*composite 2*) was followed with the notable difference that instead of a stoichiometric ratio, an excess (4 mol NH_4OH) OH/Cu ratio was

added to the suspension of functionalised MWCNTs in copper acetate hydrate solution to form the $[Cu(NH_3)_4]^{2+}$ complex (Figure 2). Figure 2 shows a scheme of the synthesis procedures.

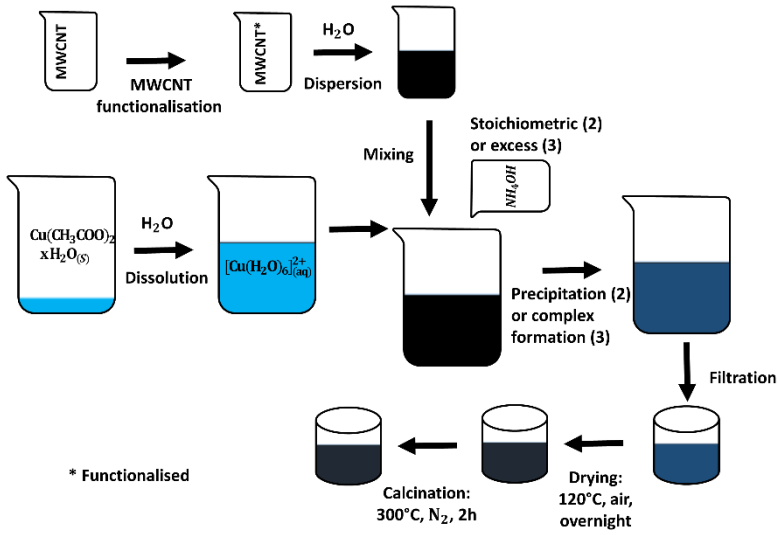

Figure 2. Scheme of the copper hydroxide precipitation (route 2) and complex attachment (route 3) synthesis procedures.

2.3. Composites characterisation

The crystalline phases of the composites were determined by means of an X-ray diffraction (XRD) (PANalytical X'Pert PROh–2h, PANalytical) scan system equipped with a Johansson monochromator (Cu Ka1 radiation, 1.5406 Å) and an X'Celerator linear detector. Crystallite sizes (S) were determined using the Scherrer equation (Patterson, 1939) (Eq. 1).

$$S = \frac{k\lambda}{\beta \cos\Theta} \quad \text{(Eq. 1)}$$

where: k – shape factor (0.9), λ – X-ray wavelength (0.15406 nm), β – full width at half-maximum intensity (radians), and θ – Bragg angle (degrees).

Transmission electron microscopy (TEM, JEOL, JEM-2200FS) was used to analyse the size and morphology of the synthesised composites. The specific surface areas (SSA) of the as-prepared composites were determined from a 5-point N_2 adsorption isotherm obtained from

Brunauer-Emmett-Teller (BET) measurements using a Beckman-Coulter SA3100 instrument. Powder samples were dried for 2 h at 180 °C in synthetic air prior to analysis.

2.4. Filter preparation To prepare the filters, 20 mg of the as-received MWCNTs or synthesised material were suspended in 20 mL of 95 % ethanol then sonicated for 5 minutes in a sonication bath. The suspension was uniformly deposited on a glass fibre filter (0.4 µm, 47 mm, Macherey-Nagel) using vacuum filtration and placed in a plastic filter holder (to support the glass fibre filter). The obtained filter loading was 1.15 mg/cm^2.

2.5. Media preparation and bacteria/ virus growth

The bacteriophages MS2 and its *Escherichia coli (E. coli)* host were purchased from the German Collection of Microorganisms and Cell Cultures (DSMZ 13767 and 5695, respectively).

MS2 bacteriophages were propagated with *E. coli* as a host, then purified and concentrated according to the DSMZ protocol (DSMZ, 2019). Briefly, MS2 were revitalised with *E. coli* solution obtaining the first stock of MS2. Subsequently, it was amplified by adding the first MS2 stock into the solution of *E. coli*. The obtained second stock was centrifuged, and then the supernatant was filtered through a 0.22 µm PES filter unit. The filtrate was collected in an autoclaved glass bottle. The last purification step consisted in filtrating the low molecular weight molecules out of the virus stock solution to increase the concentration with Amicon filters 0.22 µm (Merck).

The streptomycin solution (AppliChem), broth (tryptone soya broth, Merck), virus dilution buffer (sodium dihydrogen phosphate dihydrate (Merck), sodium chloride (VWR)), hard agar (1.5% Agar) and soft agar (0.7% Agar) (bacteriological agar, Merck) were prepared according to the Double Agar Layer (DAL) protocol (EPA, 2001).

2.6. Determination of MS2 concentration

Virus concentration was quantified using the DAL method (EPA, 2001) and was measured as a number of plaque forming unit (PFU) per mL. 100 µL of filtration permeate containing MS2 was mixed with 200 µL *E. coli* suspension and 5 mL of molten soft agar, which was then poured onto a solidified hard agar plate and incubated overnight at 37 °C.

2.7. Copper release test

After day 1 of the MS2 removal test, the as-prepared filters were rinsed with 0.01 M NaCl solution prepared with water and adjusted to pH 5 or 7 (consistent with the experimental pH) for 24 h at the same flux (160 $L/m^2 \cdot h$). Permeate samples were regularly collected and the concentration of copper released during filtration was investigated via inductively coupled plasma-mass spectrometry (ICP-MS 7500 CE, Agilent).

2.8. Virus removal experiment

The virus removal study was performed by passing the MS2 bacteriophages solution (250 mL) through the as-prepared filters at a constant flux (160 $L/m^2 \cdot h$) using a peristaltic pump. The virus solution was prepared by dilution of 250 µL of virus stock (10^{11} PFU/mL) in 250 mL of the virus dilution buffer (VDB), obtaining a final MS2 concentration of 10^8 PFU/mL. Filter permeate samples were collected and the virus concentration was determined using the DAL method. Plating was done directly after permeate collection (t=0 h), and after two hours (t=2 h) (time control) to evaluate if additional removal of virus during storage of the permeate occurred. The MS2 removal was quantified for water at both pH 5 and pH 7 and was repeated after the filter had been conditioned for 24 hours (~6 litres of water had been filtered) to test virus performance after conditioning. All experiments were performed in duplicate. MS2 $\log_{10}$ removal (LRV) was calculated using the following formula:

$$LRV = log_{10}(\frac{I_i}{I_f}) \quad \text{(Eq. 2)}$$

where: I_i - the initial MS2 concentration (PFU/mL) and I_f - the MS2 concentration in filtrate (PFU/mL).

Negative and positive controls were performed alongside each experiment, where expected results were obtained. No effect of filter permeate on the DAL assay was observed.

3. Results and discussion

3.1. Composites synthesis and characterisation

Figure 3 shows a schematic view of the interaction between the Cu species with the MWCNTs in the first step of the three different syntheses performed to fabricate the Cu_2O/ MWCNTs composites. For the copper ion attachment synthesis (route 1), due to electrostatic interactions, copper ions attach to the functional groups (-COOH, -CHO or –CO) formed on MWCNTs surface during the functionalisation step (J. Wang et al., 2013). Additionally, Cu^{2+} ions could also be adsorbed directly onto the MWCNTs surface due to opposite charges (Salam et al., 2011).

In the case of the precipitation synthesis, an addition of stoichiometric amounts of ammonia (route 2) resulted in the formation of copper(II) hydroxide precipitates (Eq. 3), which led to the formation of a composite with a higher ratio of copper species/MWCNTs in comparison with the other two syntheses routes.

In the complex attachment (route 3), the excess of ammonia led to the formation of the tetraamminediaqua copper(II) complex (Eq. 4) that reacts with the carboxylic groups of functionalised MWCNTs, leading to the amide intermediate product MWCNTs-CONH-$Cu(NH_3)_3^{2+}$ (Wang et al., 2009).

$$[Cu(H_2O)_6]^{2+}_{(aq)} + 2NH3_{(aq)} \rightarrow Cu(OH)_{2(s)} + 2NH_4^+{}_{(aq)} \quad \text{(Eq. 3)}$$

$$[Cu(H_2O)_6]^{2+}_{(aq)} + 4NH_{3(aq)} \rightarrow [Cu(NH_3)_4(H_2O)_2]^{2+}_{(aq)} + 4H_2O \quad \text{(Eq. 4)}$$

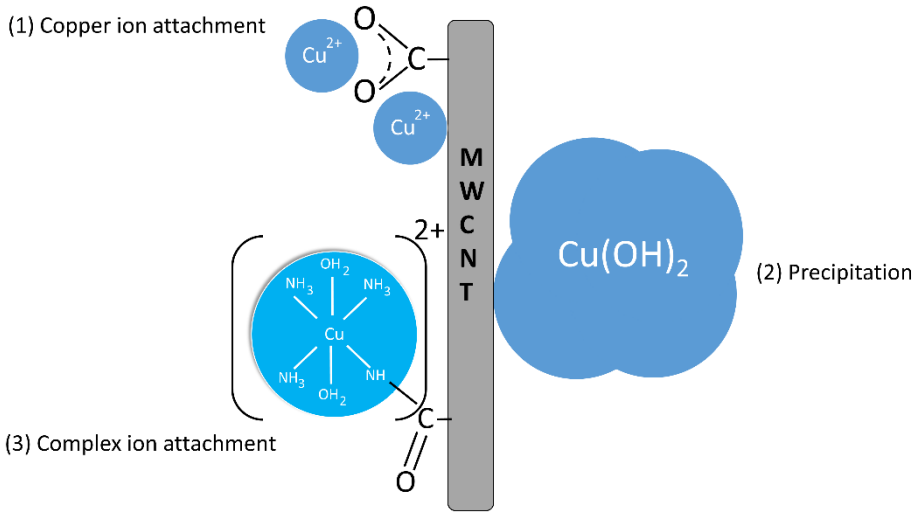

Figure 3. Scheme of the interactions of copper species with the MWCNTs during the first step of the synthesis.

The final composites formed after calcination were analysed by means of XRD in order to confirm Cu_2O-NPs presence in the composites. For all three synthesis routes, Cu_2O was obtained as a product of the synthesis, with traces of CuO in *composites 1* and *2*, as shown by XRD diffractograms (Figure 4). This result is in line with the synthesis design to improve virus removal, as Cu_2O has higher antiviral activity and lower solubility than CuO (Domagala et al., 2019a; Palmer and Bénézeth, 2008). In order to estimate the proportion between the Cu_2O and MWCNTs, the intensity ratio between the Cu_2O (I_{Cu_2O}) and C (I_C) peaks (I_{Cu_2O}/I_C ratio) was calculated, obtaining 2.3, 49.1 and 1.5 for *composite 1*, *composite 2* and *composite 3*, respectively (Table 1). The average Cu_2O crystallite sizes (calculated using the Scherrer equation) were similar (Table 1). Assuming that the amount of C is the same in all cases and that the calculated crystal sizes are similar, the changes in I_{Cu_2O}/I_C ratio are attributable to changes in Cu_2O mass. If so, *composite 2* likely has the highest I_{Cu_2O}/I_C ratio because in the precipitation synthesis all the copper precipitated as $Cu(OH)_2$. The smaller difference in I_{Cu_2O}/I_C ratio between *composite 1* and *composite 3* as the first step of the synthesis (Figure 3) is the limiting factor for the obtained Cu_2O amount in the composite. Furthermore, the free ions (Cu^{2+}) interact

with functional groups and MWCNTs surfaces with less steric and reaction limitations than in the case of the formation of the amide group between the amine complex and the MWCNTs carboxylic groups (Wang et al., 2009).

Table 1. I_{Cu2O}/I_C ratio, crystallite size, interval of nanoparticle (NP) diameter and SSA of the three synthesised composites.

Composite	I_{Cu2O}/I_C ratio	Crystallite size (nm)	NP diameter (nm)	Measured SSA (m^2/g)
1	2.3	40	12-55	207
2	49.1	36	5-85	65
3	1.5	36	8-60	215

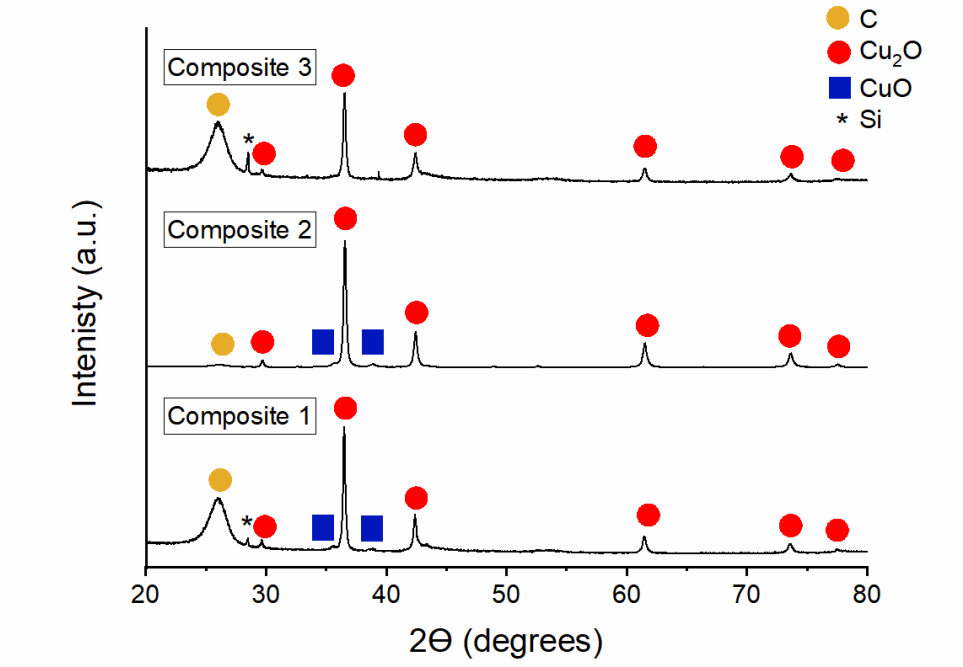

Figure 4. XRD diffractograms of obtained composites after calcination (Si peak comes from the sample holder).

TEM images of the final composites (after thermal treatment) show spherical Cu_2O nanoparticles attached to the MWCNTs (Figure 5). The NP diameters are 5-85 nm, with range varying by composite (Table 1). For *composites 1* and *3*, the single NPs appear uniformly distributed along the carbon nanotubes, whereas for *composite 2*, cuprous oxide nanoparticles agglomerated. This agglomeration is likely attributable to the high Cu_2O:MWCNTs ratio, resulting from the precipitation reaction.

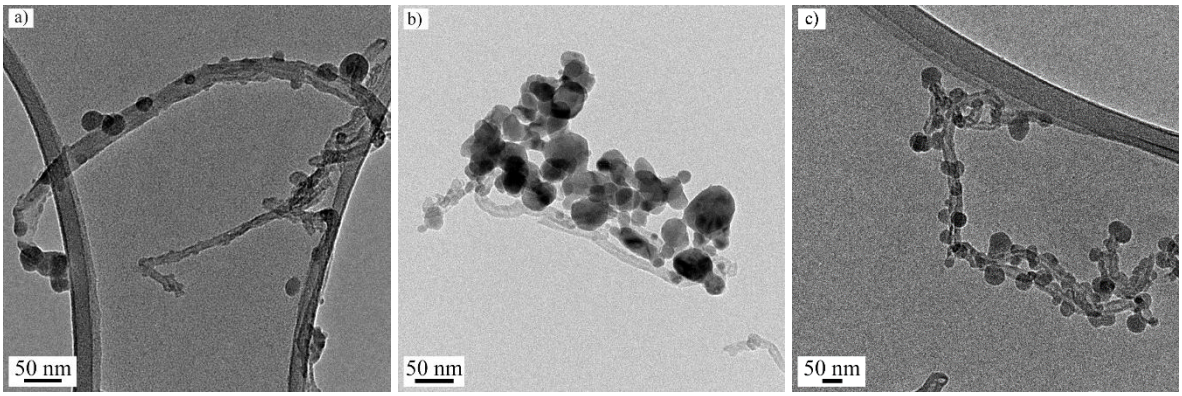

Figure 5. TEM images of obtained a) *composite 1*; b) *composite 2*; c) *composite 3*.

The high specific surface areas of the composites (Table 1) are in line with the SSA of MWCNTs, as pristine MWCNTs SSA is equal to116 m^2/g. SSA further increases during functionalisation up to 265 m^2/g, caused by the incorporation of functional groups and tube shortening (Domagala et al., 2019b). The measured values for composites follow the same trend observed in XRD patterns, i.e. the higher the intensity measured with XRD, the higher the Cu_2O amount, and the lower the SSA.

3.2. Copper dissolution tests

Copper dissolution was monitored during 24 h at pH 5 and 7 to evaluate the potential release/ dissolution of copper in the permeate to evaluate the stability of the synthesised composites. This test was essential to understand the long-term viability of the material in terms of virus removal.

Figure 6 shows the copper release experiment results at pH 5 (Figure 6a) and pH 7 (Figure 6b). Figure 6a, shows a dynamic behaviour of the copper concentration in the permeate as a function of the filtered volume for the three composites at pH 5. The concentration of copper released in the permeate for *composites 1* and *3* gradually decreases from initial concentrations of 200-400 µg/L down to <35 µg/L after the filtration of around 6 L, as shown on Figure 6a. This trend is also visible in cumulative copper mass (Figure 6c), showing permeate mass stabilised at around 1000 and 800 µg for *composite 1* and *composite 3*, respectively. In contrast, the copper release from *composite 2, depicted in Figure 6a* does not decrease until the last litre filtered , a trend also apparent in the cumulative mass of copper loss, which was nearly twice the value than for *composite 1* and *composite 3* (Figure 6c). The high dissolution may be attributable to the mass of Cu_2O-NPs, which is much higher in *composite 2* than in the others (Table 1 and Figure 6c). Moreover, for this composite the interactions between the Cu_2O-NPs and MWCNTs are expected to be weaker than in case of *composite 1*, therefore increasing the dissolution probability of Cu_2O-NPs. However, for the three composites, copper concentration in the permeate was nevertheless lower than the limit guided by the WHO for drinking water (<2 mg/L) (WHO, 2004a), and so are viable materials for filters that produce drinking water.

Our study further shows the stability of the composite being affected by pH, with clear increases in dissolution at pH 5 relative to pH 7 (Figure 6). This can be explained by the higher solubility of Cu_2O-NPs at acidic pH (4-5) as compared to neutral pH (~7) (Vargas et al., 2017; Z. Wang et al., 2013). As shown in Figure 6b, the copper concentration in the permeate of the three composites was six to seven times lower for the first flush (first few millilitres) of water filtered at pH 7 relative to the first flush at pH 5 (Figure 6a and Figure 6b). In the first flush, the copper detected in the permeate is expected to be Cu_2O-NPs, although it is not possible to exclude the presence of dissolved copper. For the three composites at pH 7, copper release dynamic was dependent on the volume filtered, with a concentration increase during the first litres of filtrated water. Over 24 hours, (approximately 6 L of filtered water), the copper mass dissolved in the

permeate reached a plateau for the three composites. Conditioning filters prior to application may therefore help rinse out excess Cu_2O-NPs, stabilising the filters. Interestingly, copper loss trend and maximum values were similar for *composite 2* and *composite 3* (Figure 6d), since both composites reached a plateau of 325 µg after filtering ~6 L through the filters. For both synthesis routes, i.e. copper hydroxide precipitation and complex ion attachment, the conditioning step results in the same copper mass loss. On the contrary, *composite 1* copper mass loss reached a maximum of 225 µg. Knowing that copper dissolution is mainly occurring at pH 5, one possible explanation concerning this behaviour difference might be that Cu_2O-NPs interactions with MWCNTs are weaker in the case of copper hydroxide precipitation and complex ion attachment syntheses routes, in comparison with the copper ion attachment one. Correlating this fact with the proposed mechanisms shown in Figure 3, for *composite 1* the direct adsorption of the Cu^{2+} on the MWCNTs surface (route 1) could lead to stronger interactions between the resulting Cu_2O-NPs and MWCNTs, since Cu_2O-NPs nucleate directly on the surface of the MWCNTs. In the case of route 2, Cu_2O-NPs were produced in excess in comparison with the MWCNTs. Therefore, the excess amount of Cu_2O-NPs are expected to be removed during the rinsing of *composite 2* filter. Furthermore, the interactions between Cu_2O-NPs are expected to be weaker than for *composite 1,* increasing the release probability of Cu_2O-NPs in *composite 2* filter permeate. For *composite 2,* NPs detachment may occur during as in the case of aliquot number 5 (Fig. 6c). Concerning route 3, the attached complexes are bonded via the amide group, which can decompose during the thermal treatment, decreasing the interaction between Cu_2O-NPs and MWCNTs and facilitating the NPs detachment. This might explain the higher stability of *composite 1* in comparison with *composite 2* and *composite 3*. However, all composites are potentially suitable in application of drinking water production, as the detected copper concentrations were 100 times below the copper limit established by the WHO.

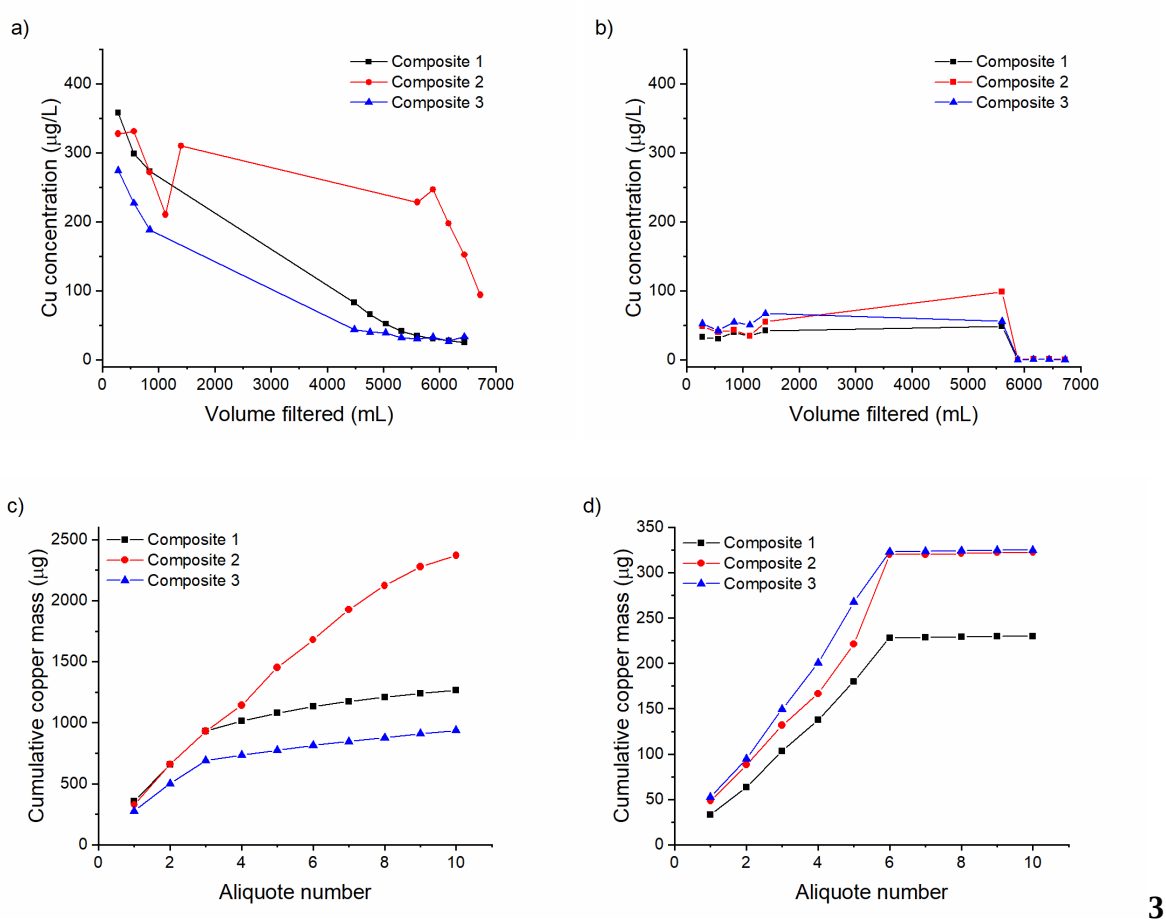

3

Figure 6. Copper dissolution test results at pH 5 (a and c) and pH 7 (b and d) of the three different composites.

3.3. Virus removal experiments

MS2 bacteriophages removal tests were performed for the first time prior to (day 1) and second time (day 2) after conditioning filters with water at pH 5 and 7 for 24 hours (Figure 7). MS2 were quantified directly after collecting the permeate (t=0 h) and again after the permeate was stored for 2 h at room temperature (t=2 h) - for "time control". This approach was established to evaluate the effect of copper dissolution on the performance of the filters.

To attest the improvement of virus removal due to MWCNTs modification with copper(I) oxide in comparison with pristine MWCNTs, MS2 solution was first filtered through a pristine MWCNTs filter. The virus removal was equal to 0.1 LRV and it remained unaffected after 2 h

384 at both pHs. This value was lower than expected, as Brady-Estévez et al. obtained up to 8 LRV
385 with MWCNTs filters, depending on the filtration conditions (Brady-Estévez et al., 2010). The
386 difference between our study and Brady-Estévez et al. might be due to (i) use of different types
387 of MWCNTs, (ii) different filtration conditions (amount of material, flux, pressure, water com-
388 position, virus-CNT contact time) and/or (iii) different filter preparation. Commercially avail-
389 able multi-walled carbon nanotubes vary greatly not only between manufacturers, but also
390 within production batches. MWCNTs differ in physical properties e.g. length, thickness, aspect-
391 ratio, chemical composition, purity level, contamination content and homogeneity (Poulsen et
392 al., 2016, 2015). These differences lead to inequalities in material biological affects and tox-
393 icity. This major difference highlights two important points: (i) pristine MWCNTs may not be
394 a relevant adsorbent for pollutants, and (ii) MS2 removal in our study is not expected to be a
395 consequence of the MWCNTs alone, but rather of the attached copper(I) oxide NPs or dissolved
396 copper. Nevertheless, in our study, the role of MWCNT was mainly to act as a network/ struc-
397 ture to support copper(I) oxide nanoparticles, the primary virucide under investigation.
398 Figure 7a shows the virus removal for the three composites as well as the copper concentrations
399 measured in the permeate after virus filtration at pH 5. The subset of tests performed on day 1
400 at t=0 h theoretically reveal virus removal due to adsorption on the filter surface, for example
401 due to MS2 electrostatic adsorption onto Cu_2O (Michen et al., 2013; Németh et al., 2019;
402 Szekeres et al., 2018; Thurman and Gerba, 1989a). The filter material is positively charged,
403 because Cu_2O is introduced onto MWCNTs surface during the synthesis process. Cu_2O pro-
404 vides positive surface charge within the tested pH range (5, 7), while the isoelectric point (IEP)
405 is in the range of 8-11 (Jing et al., 2014), leading to the conclusion that IEP of the composites
406 is also positive. The IEP of MS2 is equal to 4 (Michen and Graule, 2010; Reszka et al., 2006),
407 suggesting that adsorption is possible in our studied conditions (water pH of 5 or 7). The $\log_{10}$
408 removal was equal to 2.6, 6.1, 2.3 for the *composites 1*, *2,* and *3*, respectively, suggesting sur-
409 face adsorption of MS2. Those values were higher than the removal observed for the pristine

410 MWCNTs filter, confirming that Cu_2O-NPs composites increased virus removal. However, in
411 the t=2 h tests, the LRV increased to 5.0, >7.0 and 5.0 for *composites 1*, *2* and *3*, respectively.
412 This implies several potential virus removal mechanisms; removal at the filter surface (e.g., by
413 electrostatic adsorption) and continued virus inactivation in the permeate (e.g., due to copper
414 and Cu_2O-NPs dissolution) (Babich et al., 1980; Thurman and Gerba, 1989b). Armstrong et al.
415 have observed an additional 1.8 LRV of MS2 bacteriophage in permeate stored for 6 hours
416 containing copper concentration 7-10 times lower than in this study (Armstrong et al., 2017).
417 The increase in LRV during permeate storage highlights the need for a time control to separate
418 out LRV attributable to removal by the filter from removal due to virucidal properties of metals
419 in the permeate. Storing permeate prior to virus testing may lead to overestimates of filter per-
420 formance.

421 Virus removal at pH 5 was tested once more on day 2, after the filter was rinsed for 24 h. Again,
422 copper dissolution effect on virus removal was observed. After the conditioning step, *composite*
423 *2* still exhibited a LRV higher than 4 and an associated permeate copper concentration of
424 2.226 mg/L. This is in accordance with copper dissolution results that showed continued copper
425 dissolution from *composite 2* after 24 h conditioning. However, two statements can be made
426 for *composite 1* and *composite 3*. At day 2, t=0 h, both composites showed lower MS2 LRV
427 and lower copper concentrations in the permeate than at day 1, t=0 h. This might be explained
428 by two mechanisms; (i) the conditioning step washed out Cu_2O-NPs from filter surfaces, low-
429 ering the adsorption capacity of *composites 1* and *3* and/or (ii) at least part of the virus removal
430 is due to the direct effect of dissolved copper even at t=0 h. Second, *composites 2* and *3* exhib-
431 ited almost unchanged MS2 removal after two hours storage (6.8 to 6.8 and 0.8 to 1.0 LRV,
432 respectively), while the LRV of *composite 1* increased from 1.0 to 5.0, despite low copper con-
433 centration in the permeate (0.001 mg/L). This may indicate that other factors, apart from copper
434 concentration in the permeate, lead to increased virus removal. Amongst these factors, NPs
435 properties difference due to the different synthesis routes might also play a major role in virus

removal (Xiong et al., 2017). The ICP-MS protocol used in this study cannot differentiate between copper forms in the permeate, so further tests would be required to identify potential causes of the increased MS2 removal. However, it is possible to apply single-particle ICP-MS, which differentiates between dissolved metal ions and nanoparticles (Álvarez-Fernández García et al., 2020).

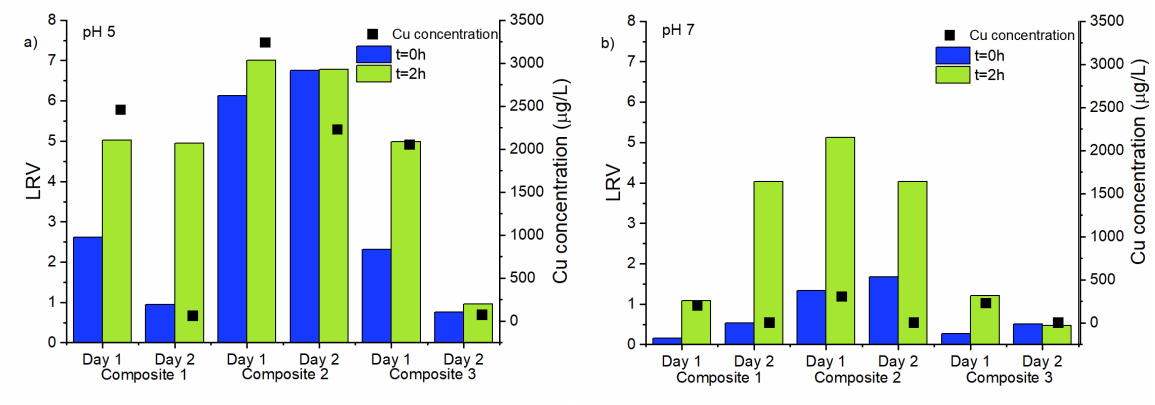

Figure 7. MS2 removal test results for *composite 1*, *composite 2* and *composite 3* at a) pH 5 and b) pH 7, and the associated copper concentrations detected in the permeate.

Figure 7b shows the results from the experiment performed at pH 7. Interestingly, at day 1 t=0 h, MS2 LRV was around 0.2-1.3 for the three composites. This is similar to the LRV observed with pristine MWCNTs and much lower than the LRV observed at pH 5. Apparent virus removal by electrostatic adsorption was therefore low for all composites. This is also in accordance with the results from Figure 7a, showing a lower removal at t=0 h when copper concentration in the permeate was lower. MS2 LRV at t=0 h is mainly explained by the immediate effect of dissolving copper, while the removal by adsorption onto the filter surface is limited.

pH 7 experiments show once again that virus removal tests for filters should account for additional virus inactivation in the permeate. At pH 7, LRV increased for day 1 t=2 h relative to t=0 h. This was surprising given that the permeate copper concentrations were low. Indeed, the MS2 LRV increased by 0.9, 3.8 and 0.9 LRV for *composites 1*, *2* and *3*, respectively, while the

associated copper concentrations were equal to 0.196, 0.301 and 0.225 mg/L. Low copper concentrations in the permeate are associated with lower MS2 LRV at t=2 h for *composite 1.* Interestingly, for *composite 1* and *composite 2* LRV increase by 3.5 and 2.3 was observed at day 2 t=2 h, despite a copper concentration of 1 µg/L in the permeate. Notably, copper concentration in the permeate was not predictive of LRV values, so including time-controlled virus removal tests should be required to assess filter efficacy.

The continued inactivation of virus in the permeate suggests copper may be virucidal in low concentrations. Although a previous work has suggested virucidal effects at concentrations of 300 µg/L (Dankovich and Smith, 2014), virucidal activity was observed here at lower concentrations. The physicochemical properties of the Cu_2O-NPs and/or interactions with MWCNTs may influence inactivation of viruses. For example, *composite 2,* has a higher ratio of Cu_2O-NPs/ MWCNTs, which facilitates/increases the probability of Cu_2O-NPs dissolution (in addition to the dissolution effect). We observed not only the immediate (t=0 h) virus inactivation due to high copper(I) oxide content but also an increase in LRV after two hours due to the above-mentioned Cu_2O-NPs dissolution.

Overall, the study results suggest that the developed composites are not sufficient to provide safe drinking water through filtration (physical removal and/or adsorption processes) alone. However, the composites provide a mechanism for virus removal through combined filtration and post-filtration virus inactivation during storage. Therefore, the developed filters may be sufficient for applications in combined treatment of filtration and post-filtration storage due to continued/ increased virus inactivation in the permeate with time, where water is stored prior to use. Importantly, the findings and the experimental procedure presented here clearly highlight the necessity to establish a procedure for (i) conditioning a filter material (for material stabilisation), (ii) proper evaluation of virus removal capacity that takes into account continued

virus inactivation in the permeate, and (iii) evaluation of the impact of the metal dissolution before using the suggested filter materials in real applications.

4. Conclusions

In this study, (nano-)Cu_2O/ MWCNTs composites were synthesised using three different syntheses routes: (1) copper ion attachment, (2) copper hydroxide precipitation and (3) $[Cu(NH_3)_4]^{2+}$ complex attachment syntheses. All three filters exhibited measurable copper dissolution (likely due to excess and/or non-bonded/weakly bonded copper particle removal, low pH influence) during water filtration, even after conditioning the filters by rinsing for 24 h. Filtered water at a lower pH (5 relative to 7) had higher copper concentrations in the permeate. Copper concentrations decreased in the permeate over time, suggesting that it may be beneficial to rinse the filters to remove excess unbound copper (conditioning) to reach material stability.

Additional virus removal was observed in the permeate when it was stored for two hours prior to virus testing. This phenomenon was observed in all three synthesised composites at both pH 5 and 7, which confirms that the electrostatic adsorption of the MS2 onto the filter is not the only mechanism involved in virus removal. Increased virus removal may be due to presence of copper (e.g., Cu_2O nanoparticles) in the permeate. However, there was no direct correlation between the copper concentration in the filtrate and the virus removal capacity. Therefore, efficiency of filter virus removal must account for continued virus removal in the permeate when virucidal compounds are incorporated into filter material. It is important to evaluate permeate composition and control the time of sample analysis, as both parameters strongly influence virus inactivation rate. Such steps can lead to improved evaluation of the responsible mechanisms behind the virus inactivation/ removal by the tested material.

5. Acknowledgements

504 Project MultiCarboVir received a private donation. Authors want to thank Dr. Sena Yüzbasi for
505 her helpful discussions.

506

507 Altintas, Z., Gittens, M., Pocock, J., Tothill, I.E., 2015. Biosensors for waterborne viruses:
508 Detection and removal. Biochimie 115, 144–154.
509 https://doi.org/10.1016/j.biochi.2015.05.010
510 Álvarez-Fernández García, R., Corte-Rodríguez, M., Macke, M., Leblanc, K.L., Mester, Z.,
511 Montes-Bayón, M., Bettmer, J., 2020. Addressing the presence of biogenic selenium
512 nanoparticles in yeast cells: Analytical strategies based on ICP-TQ-MS. Analyst 145,
513 1457–1465. https://doi.org/10.1039/c9an01565e
514 Armstrong, A.M., Sobsey, M.D., Casanova, L.M., 2017. Disinfection of bacteriophage MS2
515 by copper in water. Appl. Microbiol. Biotechnol. 101, 6891–6897.
516 https://doi.org/10.1007/s00253-017-8419-x
517 Babich, H., Stotzky, G., Ehrlich, H.L., 1980. Environmental factors that influence the toxicity
518 of heavy metal and gaseous pollutants to microorganisms. Crit. Rev. Microbiol. 8, 99–
519 145. https://doi.org/10.3109/10408418009081123
520 Brady-Estévez, A.S., Schnoor, M.H., Vecitis, C.D., Saleh, N.B., Elimelech, M., 2010.
521 Multiwalled carbon nanotube filter: Improving viral removal at low pressure. Langmuir
522 26, 14975–14982. https://doi.org/10.1021/la102783v
523 Crider, Y., Sultana, S., Unicomb, L., Davis, J., Luby, S.P., Pickering, A.J., 2018. Can you
524 taste it? Taste detection and acceptability thresholds for chlorine residual in drinking
525 water in Dhaka, Bangladesh. Sci. Total Environ. 613–614, 840–846.
526 https://doi.org/10.1016/j.scitotenv.2017.09.135
527 Dankovich, T.A., Smith, J.A., 2014. Incorporation of copper nanoparticles into paper for
528 point-of-use water purification. Water Res. 63, 245–251.
529 https://doi.org/10.1016/j.watres.2014.06.022
530 Domagala, K., Borlaf, M., Kata, M., Graule, T., 2019a. Synthesis of Copper-based Multi-
531 walled Carbon Nanotube Composites. Arch. Metall. Mater. In press.
532 Domagala, K., Borlaf, M., Traber, J., Kata, D., Graule, T., 2019b. Purification and

533 Functionalisation of Multi-Walled Carbon Nanotubes. Mater. Lett. 253, 272–275.
534 https://doi.org/doi.org/10.1016/j.matlet.2019.06.085
535 DSMZ, 2019. Supply, Storage, Propagation and Purification of Phages [WWW Document].
536 URL
537 https://www.dsmz.de/fileadmin/user_upload/Collection_allg/Special_Instruction_Phages
538 .pdf (accessed 10.18.19).
539 Elsehly, E.M., Chechenin, N.G., Makunin, A. V., Shemukhin, A.A., Motaweh, H.A., 2018.
540 Enhancement of CNT-based filters efficiency by ion beam irradiation. Radiat. Phys.
541 Chem. 146, 19–25. https://doi.org/10.1016/j.radphyschem.2018.01.007
542 EPA, 2001. Method 1602 : Male-specific (F +) and Somatic Coliphage in Water by Single
543 Agar Layer (SAL) Procedure April 2001. EPA Document 821-R-01-029.
544 Fischer Walker, C.L., Rudan, I., Liu, L., Nair, H., Theodoratou, E., Bhutta, Z.A., O'Brien,
545 K.L., Campbell, H., Black, R.E., 2013. Global burden of childhood pneumonia and
546 diarrhoea. Lancet 381, 1405–1416. https://doi.org/10.1016/S0140-6736(13)60222-6
547 Gall, A.M., Mariñas, B.J., Lu, Y., Shisler, J.L., 2015. Waterborne Viruses: A Barrier to Safe
548 Drinking Water. PLOS Pathog. 11. https://doi.org/10.1371/journal.ppat.1004867
549 Gibson, K.E., Opryszko, M.C., Schissler, J.T., Guo, Y., Schwab, K.J., 2011. Evaluation of
550 human enteric viruses in surface water and drinking water resources in southern Ghana.
551 Am. J. Trop. Med. Hyg. 84, 20–29. https://doi.org/10.4269/ajtmh.2011.10-0389
552 Guo, D.J., Li, H.L., 2005. High dispersion and electrocatalytic properties of platinum on
553 functional multi-walled carbon nanotubes. Electroanalysis 17, 869–872.
554 https://doi.org/10.1002/elan.200403164
555 Jing, H.Y., Wen, T., Fan, C.M., Gao, G.Q., Zhong, S.L., Xu, A.W., 2014. Efficient
556 adsorption/photodegradation of organic pollutants from aqueous systems using Cu2O
557 nanocrystals as a novel integrated photocatalytic adsorbent. J. Mater. Chem. A 2, 14563–
558 14570. https://doi.org/10.1039/c4ta02459a

559 Kim, J.P., Kim, J.H., Kim, J., Lee, S.N., Park, H.O., 2016. A nanofilter composed of carbon
560 nanotube-silver composites for virus removal and antibacterial activity improvement. J.
561 Environ. Sci. (China). https://doi.org/10.1016/j.jes.2014.11.017
562 Lantagne, D., Clasen, T., 2013. Effective use of household water treatment and safe storage in
563 response to the 2010 haiti earthquake. Am. J. Trop. Med. Hyg. 89, 426–433.
564 https://doi.org/10.4269/ajtmh.13-0179
565 Liu, L., Oza, S., Hogan, D., Perin, J., Rudan, I., Lawn, J.E., Cousens, S., Mathers, C., Black,
566 R.E., 2015. Global, regional, and national causes of child mortality in 2000-13, with
567 projections to inform post-2015 priorities: An updated systematic analysis. Lancet 385,
568 430–440. https://doi.org/10.1016/S0140-6736(14)61698-6
569 Mallakpour, S., Khadem, E., 2016. Carbon nanotube–metal oxide nanocomposites:
570 Fabrication, properties and applications. Chem. Eng. J. 302, 344–367.
571 https://doi.org/10.1016/j.cej.2016.05.038
572 Michen, B., Fritsch, J., Aneziris, C., Graule, T., 2013. Improved virus removal in ceramic
573 depth filters modified with MgO. Environ. Sci. Technol. 47, 1526–1533.
574 https://doi.org/10.1021/es303685a
575 Michen, B., Graule, T., 2010. Isoelectric points of viruses. J. Appl. Microbiol.
576 https://doi.org/10.1111/j.1365-2672.2010.04663.x
577 Németh, Z., Szekeres, G.P., Schabikowski, M., Schrantz, K., Traber, J., Pronk, W., Hernádi,
578 K., Graule, T., 2019. Enhanced virus filtration in hybrid membranes with MWCNT
579 nanocomposite. R. Soc. Open Sci. 6, 181294. https://doi.org/10.1098/rsos.181294
580 Ngoc Dung, T.T., Phan Thi, L.A., Nam, V.N., Nhan, T.T., Quang, D.V., 2019. Preparation of
581 silver nanoparticle-containing ceramic filter by in-situ reduction and application for
582 water disinfection. J. Environ. Chem. Eng. 7, 103176.
583 https://doi.org/10.1016/j.jece.2019.103176
584 Ong, Y.T., Ahmad, A.L., Zein, S.H.S., Tan, S.H., 2010. A review on carbon nanotubes in an

environmental protection and green engineering perspective. Brazilian J. Chem. Eng. 27, 227–242. https://doi.org/10.1590/S0104-66322010000200002

Oyanedel-Craver, V.A., Smith, J.A., 2008. Sustainable colloidal-silver-impregnated ceramic filter for point-of-use water treatment. Environ. Sci. Technol. 42, 927–933. https://doi.org/10.1021/es071268u

Palmer, D.A., Bénézeth, P., 2008. Solubility of Copper Oxides in Water and Steam, in: 14Th International Conference on the Properties of Water and Steam in Kyoto. pp. 491–496.

Patterson, A.L., 1939. The scherrer formula for X-ray particle size determination. Phys. Rev. 56, 978–982. https://doi.org/10.1103/PhysRev.56.978

Peter-Varbanets, M., Zurbrügg, C., Swartz, C., Pronk, W., 2009. Decentralized systems for potable water and the potential of membrane technology. Water Res. 43, 245–265. https://doi.org/10.1016/j.watres.2008.10.030

Poulsen, S.S., Jackson, P., Kling, K., Knudsen, K.B., Skaug, V., Kyjovska, Z.O., Thomsen, B.L., Clausen, P.A., Atluri, R., Berthing, T., Bengtson, S., Wolff, H., Jensen, K.A., Wallin, H., Vogel, U., 2016. Multi-walled carbon nanotube physicochemical properties predict pulmonary inflammation and genotoxicity. Nanotoxicology 10, 1263–1275. https://doi.org/10.1080/17435390.2016.1202351

Poulsen, S.S., Saber, A.T., Williams, A., Andersen, O., Købler, C., Atluri, R., Pozzebon, M.E., Mucelli, S.P., Simion, M., Rickerby, D., Mortensen, A., Jackson, P., Kyjovska, Z.O., Mølhave, K., Jacobsen, N.R., Jensen, K.A., Yauk, C.L., Wallin, H., Halappanavar, S., Vogel, U., 2015. MWCNTs of different physicochemical properties cause similar inflammatory responses, but differences in transcriptional and histological markers of fibrosis in mouse lungs. Toxicol. Appl. Pharmacol. 284, 16–32. https://doi.org/10.1016/j.taap.2014.12.011

Qin, X., Gao, X., Liu, H., Yoan, H., 2000. Electrochemical Hydrogen Storage of Multiwalled Carbon Nanotubes. Electrochem. Solid-State Lett. 3, 532–535.

Rahaman, M.S., Vecitis, C.D., Elimelech, M., 2012. Electrochemical carbon-nanotube filter performance toward virus removal and inactivation in the presence of natural organic matter. Environ. Sci. Technol. 46, 1556–1564. https://doi.org/10.1021/es203607d

Rajarao, R., Jayanna, R.P., Sahajwalla, V., Bhat, B.R., 2014. GreenApproach to Decorate Multi-walled Carbon Nanotubes by Metal/Metal Oxide Nanoparticles. Procedia Mater. Sci. 5, 69–75. https://doi.org/10.1016/j.mspro.2014.07.243

Rao, G., Brastad, K.S., Zhang, Q., Robinson, R., He, Z., Li, Y., 2016. Enhanced disinfection of Escherichia coli and bacteriophage MS2 in water using a copper and silver loaded titanium dioxide nanowire membrane. Front. Environ. Sci. Eng. 10. https://doi.org/10.1007/s11783-016-0854-x

Reszka, M., Janusz, W., Gałgan, A., 2006. Electrical double layer the Cu2O/aqueous solution of alkali metal chlorides interface. Physicochem. Probl. Miner. Process. 40, 161–174.

Salam, M.A., Makki, M.S.I., Abdelaal, M.Y.A., 2011. Preparation and characterization of multi-walled carbon nanotubes/chitosan nanocomposite and its application for the removal of heavy metals from aqueous solution. J. Alloys Compd. 509, 2582–2587. https://doi.org/10.1016/j.jallcom.2010.11.094

Salsali, H., McBean, E., Brunsting, J., 2011. Virus removal efficiency of Cambodian ceramic pot water purifiers. J. Water Health 9, 306–311. https://doi.org/10.2166/wh.2011.087

Sarkar, B., Mandal, S., Tsang, Y.F., Kumar, P., Kim, K.H., Ok, Y.S., 2018. Designer carbon nanotubes for contaminant removal in water and wastewater: A critical review. Sci. Total Environ. 612, 561–581. https://doi.org/10.1016/j.scitotenv.2017.08.132

Satishkumar, B.C., Govindaraj, A., Nath, M., Rao, C.N.R., 2000. Synthesis of metal oxide nanorods using carbon nanotubes as templates. J. Mater. Chem. 10, 2115–2119. https://doi.org/10.1039/b002868l

Shimabuku, Q.L., Arakawa, F.S., Fernandes Silva, M., Ferri Coldebella, P., Ueda-Nakamura, T., Fagundes-Klen, M.R., Bergamasco, R., 2017. Water treatment with exceptional virus

637 inactivation using activated carbon modified with silver (Ag) and copper oxide (CuO)
638 nanoparticles. Environ. Technol. (United Kingdom) 38, 2058–2069.
639 https://doi.org/10.1080/09593330.2016.1245361
640 Sirikanchana, K., Shisler, J.L., Mariñas, B.J., 2008. Effect of exposure to UV-C irradiation
641 and monochloramine on adenovirus serotype 2 early protein expression and DNA
642 replication. Appl. Environ. Microbiol. 74, 3774–3782.
643 https://doi.org/10.1128/AEM.02049-07
644 Szekeres, G.P., Nemeth, Z., Schrantz, K., Nemeth, K., Schabikowski, M., Traber, J., Pronk,
645 W., Hernadi, K., Graule, T., 2018. Copper-Coated cellulose-based water filters for virus
646 retention. ACS Omega 3, 446–454. https://doi.org/10.1021/acsomega.7b01496
647 Thurman, R.B., Gerba, C.P., 1989a. The molecular mechanisms of copper and silver ion
648 disinfection of bacteria and viruses. Crit. Rev. Environ. Control 18, 295–315.
649 https://doi.org/10.1080/10643388909388351
650 Thurman, R.B., Gerba, C.P., 1989b. The molecular mechanisms of copper and silver ion
651 disinfection of bacteria and viruses. Crit. Rev. Environ. Control 18, 295–315.
652 https://doi.org/10.1080/10643388909388351
653 Trompeta, A.F., Koklioti, M.A., Perivoliotis, D.K., Lynch, I., Charitidis, C.A., 2016. Towards
654 a holistic environmental impact assessment of carbon nanotube growth through chemical
655 vapour deposition. J. Clean. Prod. 129, 384–394.
656 https://doi.org/10.1016/j.jclepro.2016.04.044
657 UNICEF, WHO, 2019. Progress on household drinking water, sanitation and hygiene 2000-
658 2017. Special focus on inequalities., Progress on Drinking Water, Sanitation and
659 Hygiene 2000-2017.
660 United States Environmental Protection Agency, n.d. Drinking Water Contaminants –
661 Standards and Regulations [WWW Document]. URL
662 https://www.epa.gov/dwstandardsregulations (accessed 11.15.19).

663 Van der Laan, H., van Halem, D., Smeets, P.W.M.H., Soppe, A.I.A., Kroesbergen, J.,
664 Wubbels, G., Nederstigt, J., Gensburger, I., Heijman, S.G.J., 2014. Bacteria and virus
665 removal effectiveness of ceramic pot filters with different silver applications in a long
666 term experiment. Water Res. 51, 47–54. https://doi.org/10.1016/j.watres.2013.11.010
667 Vargas, I.T., Fischer, D.A., Alsina, M.A., Pavissich, J.P., Pablo, P., Pizarro, G.E., 2017.
668 Copper corrosion and biocorrosion events in premise plumbing. Materials (Basel). 10, 1–
669 30. https://doi.org/10.3390/ma10091036
670 Wang, J., Li, Z., Li, S., Qi, W., Liu, P., Liu, F., Ye, Y., Wu, L., Wang, L., Wu, W., 2013.
671 Adsorption of Cu(II) on Oxidized Multi-Walled Carbon Nanotubes in the Presence of
672 Hydroxylated and Carboxylated Fullerenes. PLoS One 8.
673 https://doi.org/10.1371/journal.pone.0072475
674 Wang, W., Serp, P., Kalck, P., Faria, J.L., 2005. Photocatalytic degradation of phenol on
675 MWNT and titania composite catalysts prepared by a modified sol-gel method. Appl.
676 Catal. B Environ. 56, 305–312. https://doi.org/10.1016/j.apcatb.2004.09.018
677 Wang, X., Zhang, F., Xia, B., Zhu, X., Chen, J., Qiu, S., Zhang, P., Li, J., 2009. Controlled
678 modification of multi-walled carbon nanotubes with CuO, Cu2O and Cu nanoparticles.
679 Solid State Sci. 11, 655–659. https://doi.org/10.1016/j.solidstatesciences.2008.10.009
680 Wang, Z., Von Dem Bussche, A., Kabadi, P.K., Kane, A.B., Hurt, R.H., 2013. Biological and
681 environmental transformations of copper-based nanomaterials. ACS Nano 7, 8715–8727.
682 https://doi.org/10.1021/nn403080y
683 Wani, W.A., Prashar, S., Shreaz, S., Gómez-Ruiz, S., 2016. Nanostructured materials
684 functionalized with metal complexes: In search of alternatives for administering
685 anticancer metallodrugs. Coord. Chem. Rev. 312, 67–98.
686 https://doi.org/10.1016/j.ccr.2016.01.001
687 WHO, 2017. Guidelines for drinking water quality.
688 WHO, 2004a. Copper in Drinking-water, WHO/SDE/WSH/03.04/88.

https://doi.org/10.1111/1467-8292.00035

WHO, 2004b. Guidelines for Drinking-water Quality Third Edition. Geneva.

Wood, L., 2018. ResearchAndMarkets.com, Global Nanotubes Market - Segmented by Product type, Application, End-user Industry and Region - Growth, Trends, and Forecast (2018 – 2023) [WWW Document]. URL https://www.businesswire.com/news/home/20180509006235/en/Global-Nanotubes-Market-2018-Forecast-2023--, published 05.2018, accessed 27.11.2019 (accessed 11.27.19).

Xiong, L., Yu, H., Nie, C., Xiao, Y., Zeng, Q., Wang, G., Wang, B., Lv, H., Li, Q., Chen, S., 2017. Size-controlled synthesis of Cu2O nanoparticles: Size effect on antibacterial activity and application as a photocatalyst for highly efficient H2O2 evolution. RSC Adv. 7, 51822–51830. https://doi.org/10.1039/c7ra10605j